



Audio Engineering Society Convention Paper

Presented at the 110th Convention
2001 May 12–15 Amsterdam, The Netherlands

This convention paper has been reproduced from the author's advance manuscript, without editing, corrections, or consideration by the Review Board. The AES takes no responsibility for the contents. Additional papers may be obtained by sending request and remittance to Audio Engineering Society, 60 East 42nd Street, New York, New York 10165-2520, USA; also see www.aes.org. All rights reserved. Reproduction of this paper, or any portion thereof, is not permitted without direct permission from the Journal of the Audio Engineering Society.

“Horn’s Directivity Related to the Pressure Distribution at their Mouth: part 2”

Mario Di Cola, Davide Doldi, and Davide Saronni

AES Members

20100 Milano,
Italy

e-mail: mario.di.col@usa.net, davide.doldi@tiscalinet.it, il_digital@tin.it

0. ABSTRACT

The directional properties of horn devices are governed by the wavefront’s shape presented at the mouth.

An analysis of the sound pressure distribution across the horn’s mouth that we call Pressure Distribution Mapping could certainly be helpful to understand how the wavefront is shaped there.

Moreover, this could help to understand what happens in some particular circumstances.

For example midrange beaming or high frequency mouth diffraction phenomena are two well known obstacles to overcome designing a broad band constant directivity horn.

The method forwarded by us in the previous work is here extended to some different cases and improved in the data processing.

The results that come out of such analysis will be shown through graphic illustrations.

Presented will be the results obtained performing measurements upon real devices correlated to traditional directivity plots as well.

1. BACKGROUND

The analysis we are going to show here has just demonstrated its proven usefulness. In fact, in order to understand the origin of unexpected behaviours that give to horns many problems in directivity controlling, we found really helpful in horn design to take a look at what kind of distribution, at the horn's mouth, the pressure assumes at various frequencies. This could be useful to understand why that horn behave in a particular way. Some tools are traditionally widely used in directivity performances analysis. These tools are well known amongst designers and users. These are Polar plots (Fig.1), Beamwidth and Directivity Index plots (Fig. 2 & Fig. 3), Isobars in polar or rectangular coordinates (Fig. 4 & Fig. 5), Waterfall Polar plots (Fig. 6) and Directivity Color Map (Fig. 7). All these analysis tools show a collection of Pressure Magnitude data (sometimes Phase as well) measured in some portion of the space (sometimes the whole space) around the source. They are absolutely fundamental in studying directivity of the source, but because of their intrinsic nature, they only show "how" a device behaves.

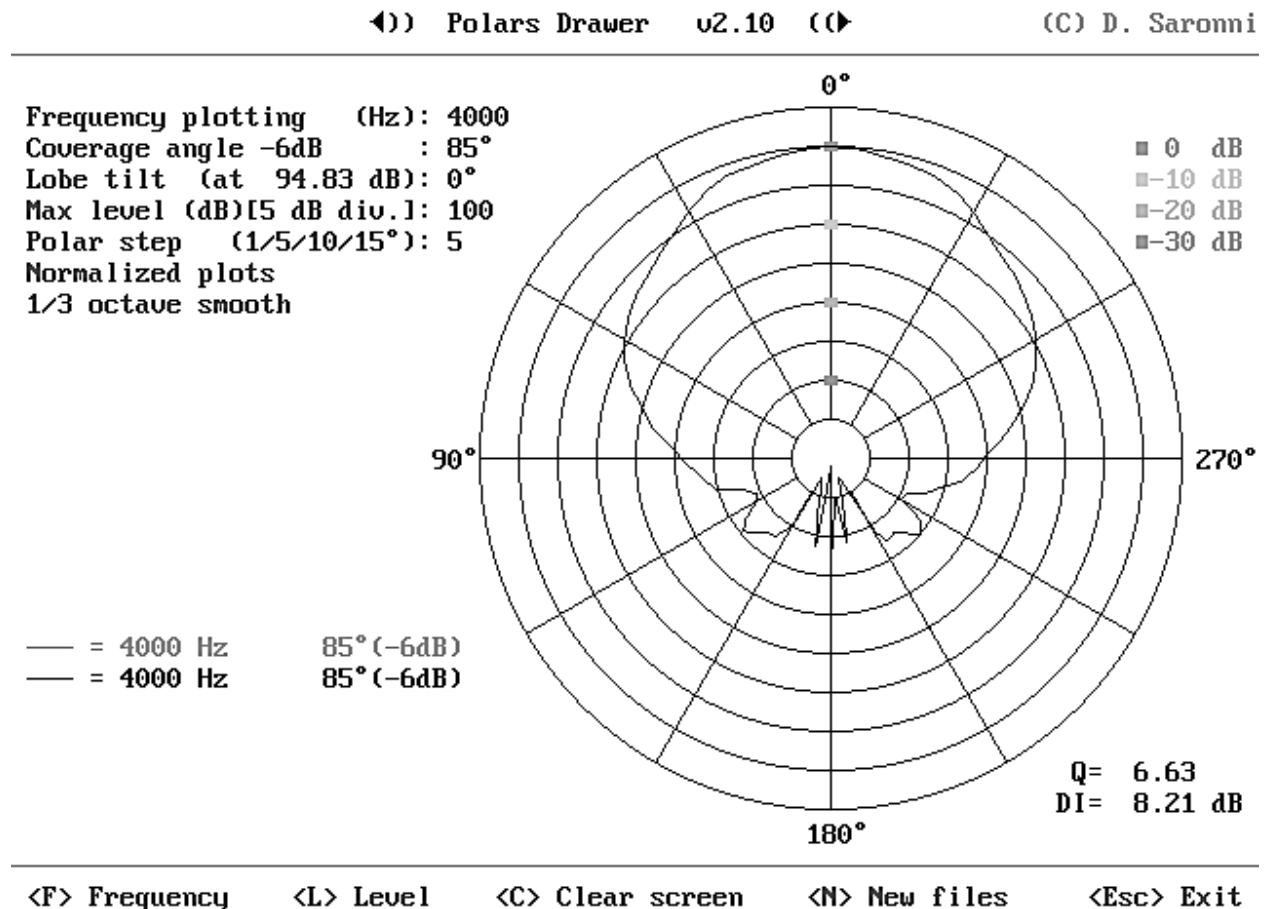


Figure 1: An example of Polar Plot

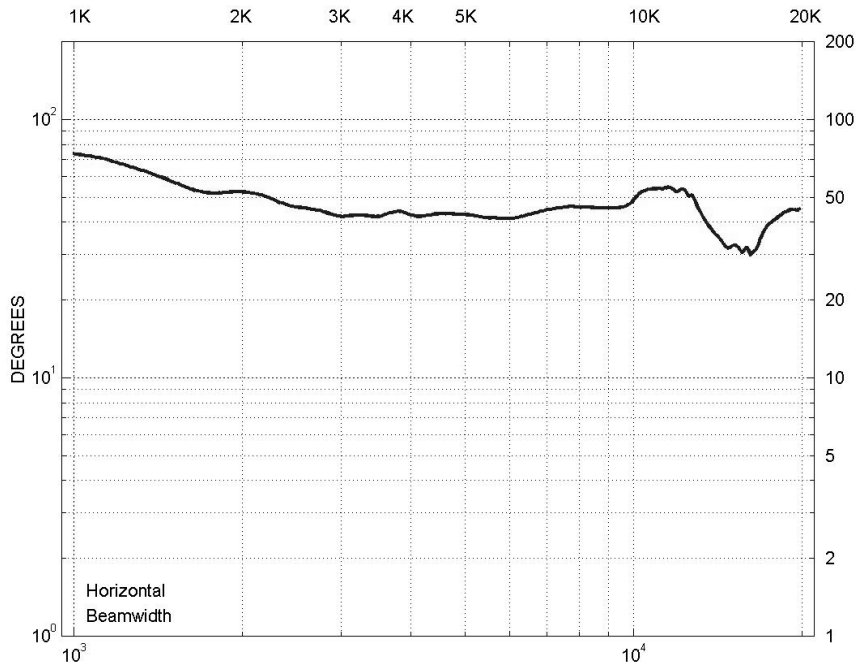


Figure 2: An example of Beamwidth plot

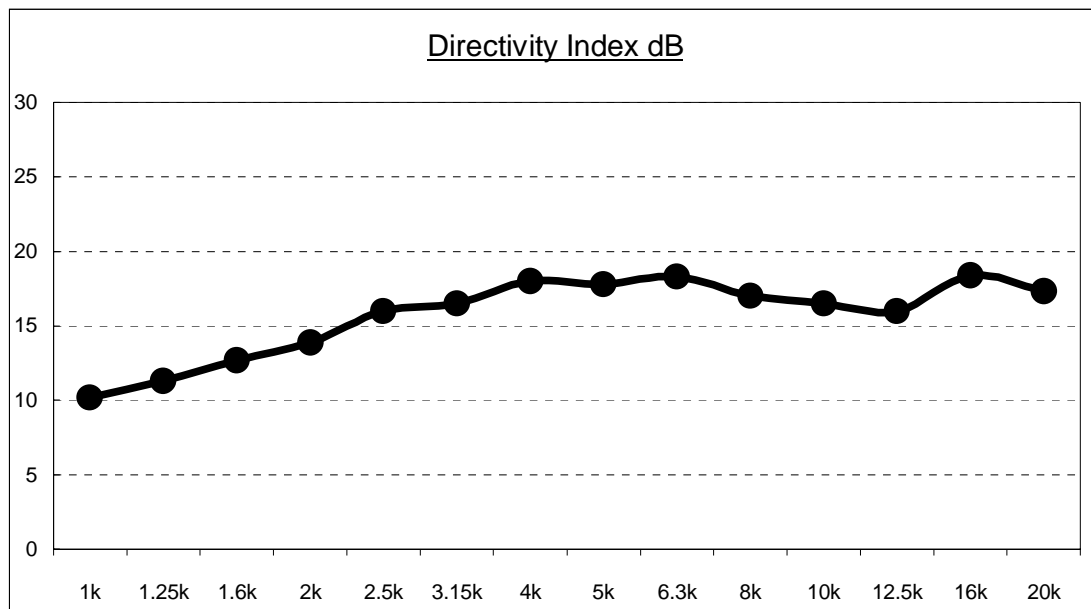


Figure 3: An example of Directivity Index plot

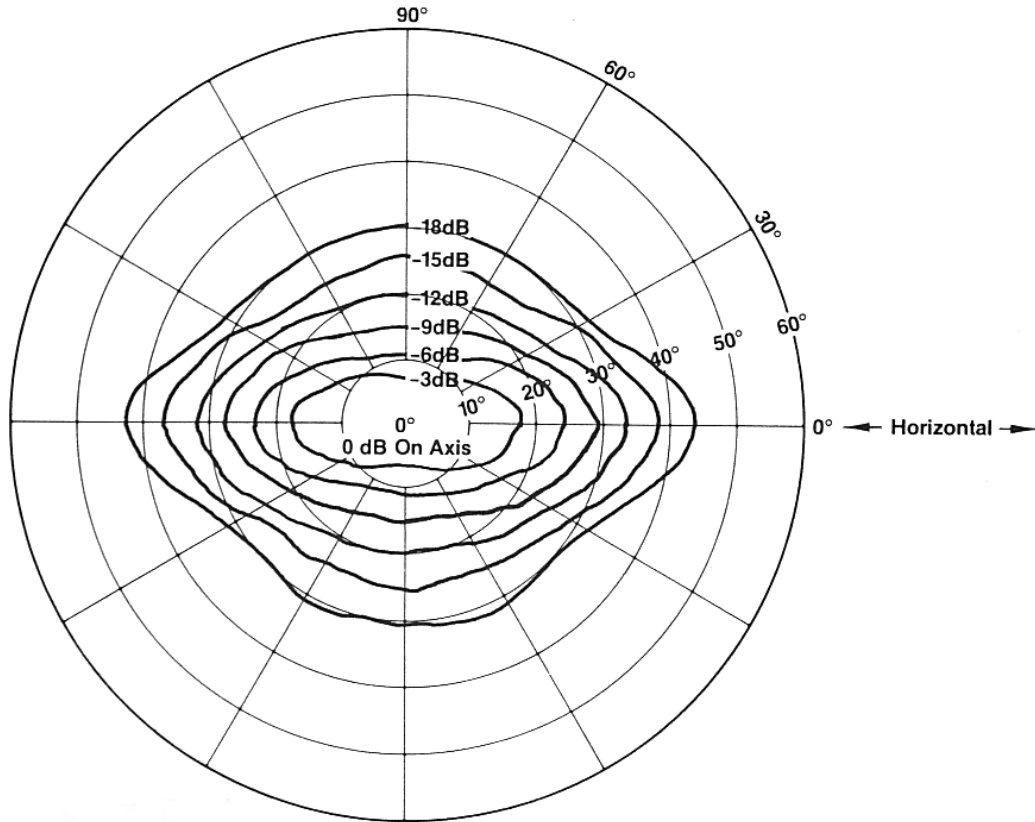


Figure 4: An example of Isobar plot in polar coordinates (from a JBL Whitepaper)

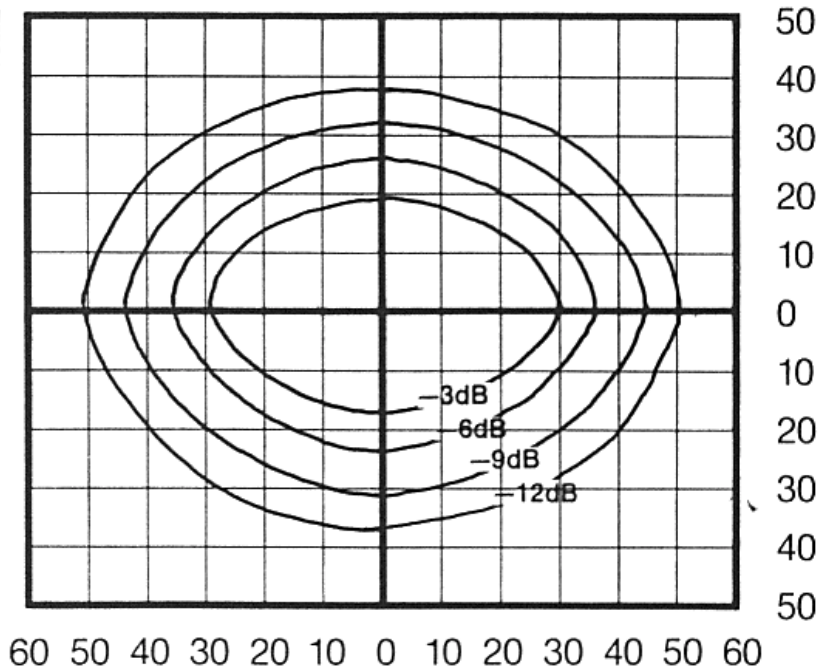


Figure 5: An example of Isobar plot in rectangular coordinates (from a JBL Whitepaper)

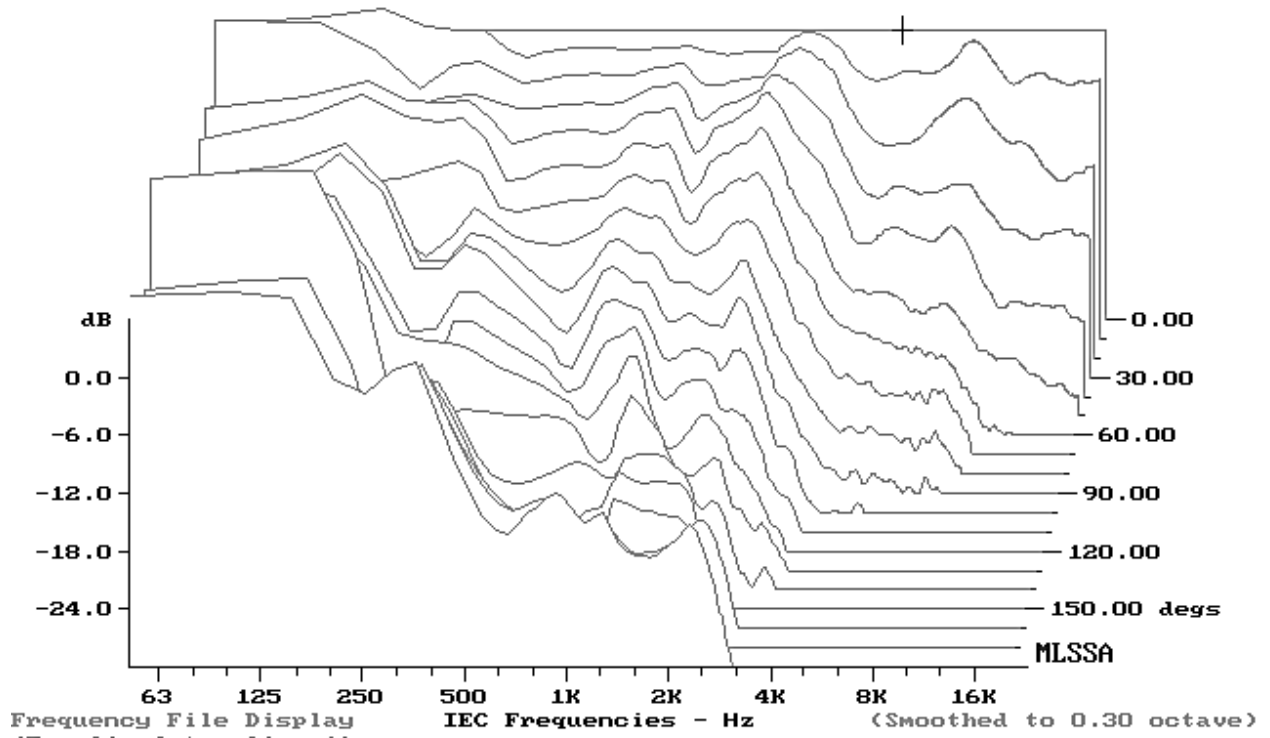


Figure 6: An example of Waterfall Polar normalized plot

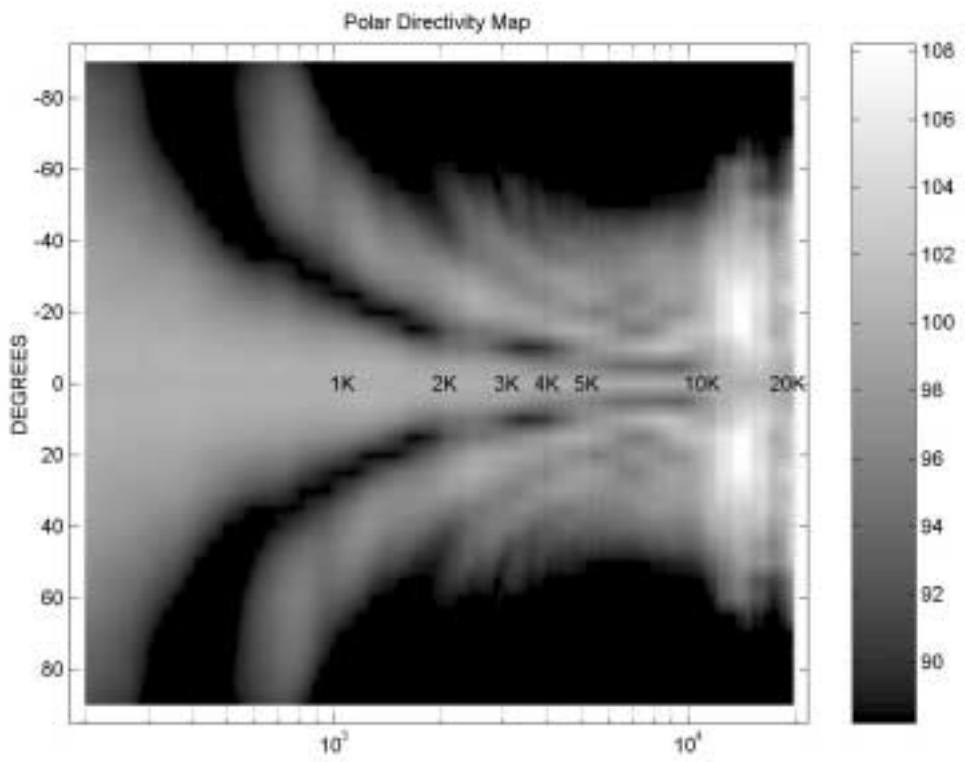


Figure 7: An example of Directivity Color Map normalized plot

Adding to those one more information that tell us something about “why” it behaves like that, could help us to have a more complete idea of the situation while studying an horn/waveguide. So, the study of the distribution that the sound pressure assumes at the horn's mouth could help to understand this.

Don B. Keele for example, in his famous work [1] about constant directivity CE horns showed the seriousness of the midrange beaming effect.

He pointed out the fact that, by flaring in an opportune way the final part of the horn, this problem could be worked out and that the actual behaviour of the horn could be investigated by collecting amplitude measurements across the horn's mouth.

He explained as the mouth's pressure distribution can give an indication of what is the effective size of the acoustic source.

Moreover, performing a complete set of Impulse Response measurement throughout the mouth's surface with one of the known techniques, say MLS for example, we can even collect time arrival information that could help us to even reconstruct (with some approximations) how the wavefront is shaped at the horn's mouth. This, could be even shown as a function of the frequency. Related to horn's mouth another very important work was made by E. Geddes [2], that gave an explanation of which phenomena are at the origin of mouth diffraction effects and showed even that when we have a known velocity distribution at the horn's mouth, the far field pressure can be calculated.

3. CONSTANT DIRECTIVITY IN HORNS AND WAVEGUIDES DESIGN

Every loudspeaker systems engineer that use horn loudspeakers probably have found that the directional properties of realworld horns and waveguides generally disagree from the theoretical behaviour or at least from the expected ones.

Almost in all cases their directivity depends on frequency. They get very close to the expectations at some frequencies and, they are far away from those at some other frequencies.

It could be clearly shown that something unexpected happens depending on frequency.

In fact, as largely agreed from all the theory reviewers about this topic, through a waveguide having a conical shaped profile the wavefront propagates itself spherically shaped, straight to the mouth and to the external environment, and this wavefront must be everytime perpendicular to the wall surfaces of the waveguide. Generally speaking every time we would get constant directivity we should use an horn profile that is perpendicular to the wavefront we would let propagate [3].

The problem is that all the waveguides in the real world are finite in dimensions (with no exception!) and this is the most important cause of the disagreement with the theory.

Horn's theory in fact, in order to be not too much complicated, needs to consider as a starting point that the horn itself should be considered infinite.

For real world horns, their dimensions at very high frequencies may let the horn behave quite close as it would be infinite, but other kind of problems arise anyway and these prevent the horn to act as the theory asserts as well.

The most important issues related to the obtaining of constant directivity behaviour in real horns are mainly the midrange beaming (Fig. 8) and high frequencies diffraction effects (Fig.9).

But maybe that we could highlight other kind of problems related to some beamwidth and directivity index discontinuities as well.

For example another important undesirable directivity behaviour is represented by the “waist-banding effect”.

This problem was widely pointed out from M. Ureda and C. Henricksen in their works about Mantaray horns [4a][4b].

To quote: “ It seems somewhere in the mid frequencies, just above the beaming frequencies, the horns will tend to lose a lot of energy out of the sides.

This shows up as lobes in the polar response curves” (Fig. 10)

Some solutions in order to work out all these problems are however available.

For example, in a previous work of ours [5] we pointed out, proving with practical measurements, what kind of improvement could be obtained shaping accurately the horn's mouth in terms of high frequency diffraction effects.

But a mouth flaring that tends in the last part of the horn to augment the included angle shows its beneficial effect even in minimizing midrange narrowing phenomenon.

Waisting band effect could be minimized as well by designing properly the mouth.

Ureda and Henricksen showed off radial horn design suffers from this problem for example more than other designs.

A complete picture of the whole directivity performances of an horn could be better resumed in a above mentioned color (or gray scale) map that could show throughout the entire working band (with very fine resolution) the ability of the device in controlling energy in a plane.

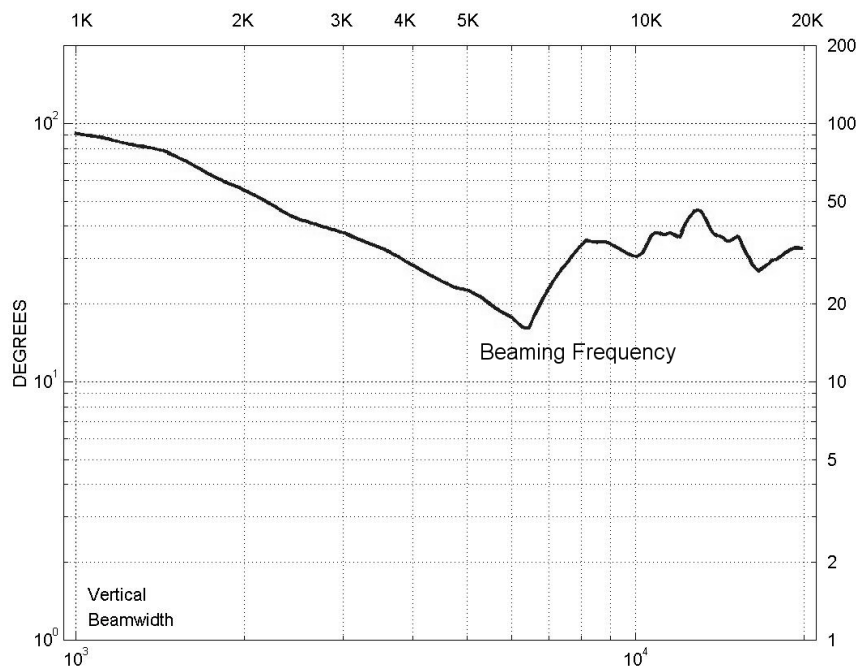


Fig. 8: An example of a Beaming problem at about 6.3 kHz

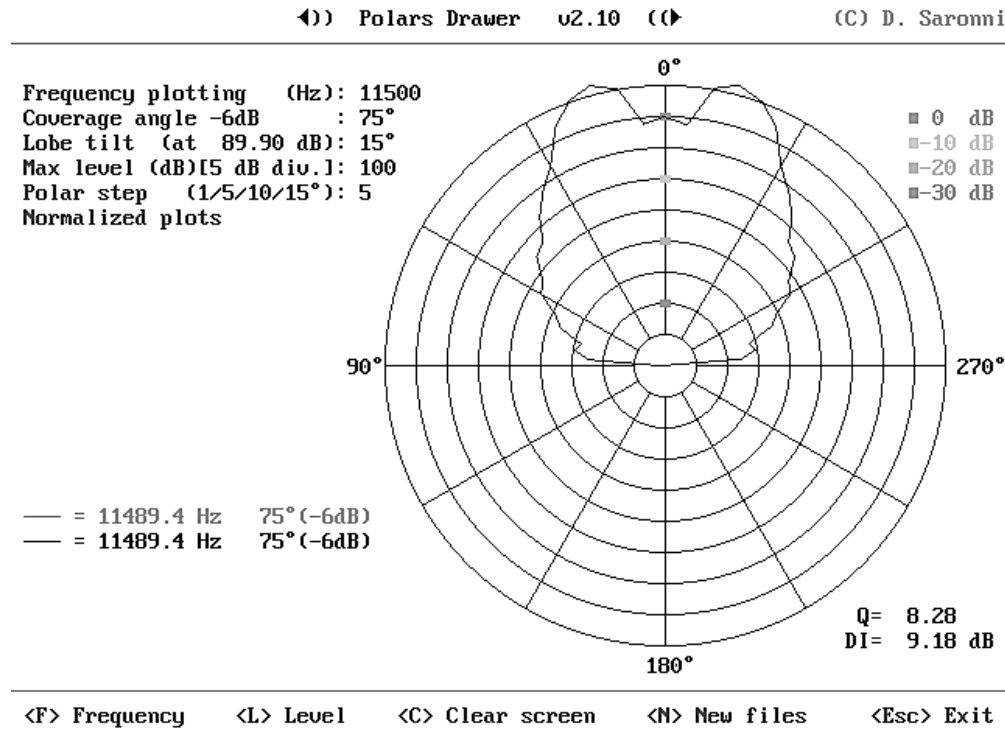


Fig. 9: An example of a Diffraction problem at very high frequency

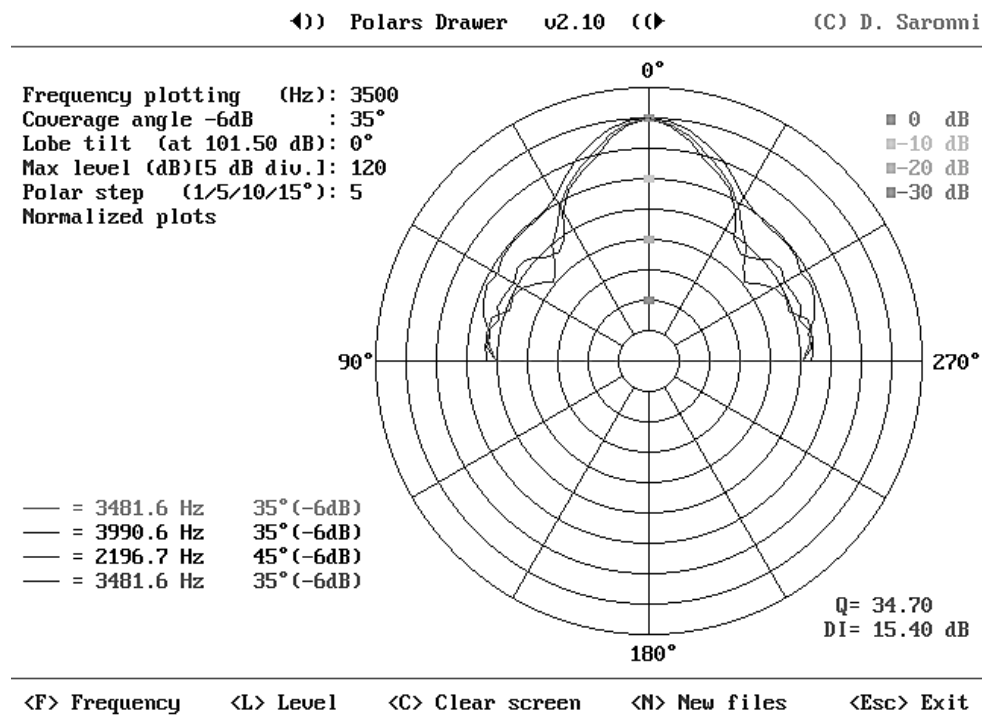


Fig. 10: An example of Waist-band energy problem

As cited before, constant directivity performances on high frequency horns is a great deal of discussion and researching for almost every professional loudspeaker system's engineer. But we even know that some obstacles need to be overcome to get constant directivity. In real world professional high power systems suited for sound reinforcement, compression drivers are usually employed. They are usually coupled to small format horns in order to get the most compact dimensions to the system.

The fundamental issues related to constant directivity performances in such systems can be:

- The profile of the horn/waveguide: it should allow the horn to be theoretically a constant directivity device.
- Due to the finite dimensions of the horn/waveguide some modification of the theoretical profile should be used to minimize midrange beaming and high band diffraction effects.
- Understanding of which behaviour depends from which part of the horn [6].
- Driver-waveguide flare and shape matching [7] at the driver's exit with a perfect suited throat.
- Driver exit diameter as a cause of very high frequency beaming.
- Driver's wavefront coherence due to the phase plug geometries.
- Driver's behaviour at high frequencies and particularly the exit's coherence at the break-up frequencies: effects due to the vibration resonances of the diaphragms [8].

So, each time we are involved designing an horn, particularly if it's an high frequency horn, these are some very important issues we should think about, and their optimizing process is usually a very difficult matter.

We found the analysis tool used here to be very useful to understand what should be worked out to improve directivity performances of any new horn, or investigate the anomalies of existing designs.

4. MEASUREMENT METHOD

As we have just said in the part 1 of the paper, the technique we used to perform such analysis could be considered very trivial, and ...definitely it is!

We divided the mouth's surface of any horn with a grid made of very very thin nylon thread.

Each square element had the dimension of 1 cm (less that $\frac{1}{2}$ inch).

We took 3 averaged measurement in the center of each square element using a MLS measurement system.

The microphones used is an $\frac{1}{4}$ inch one. (Fig. 11)

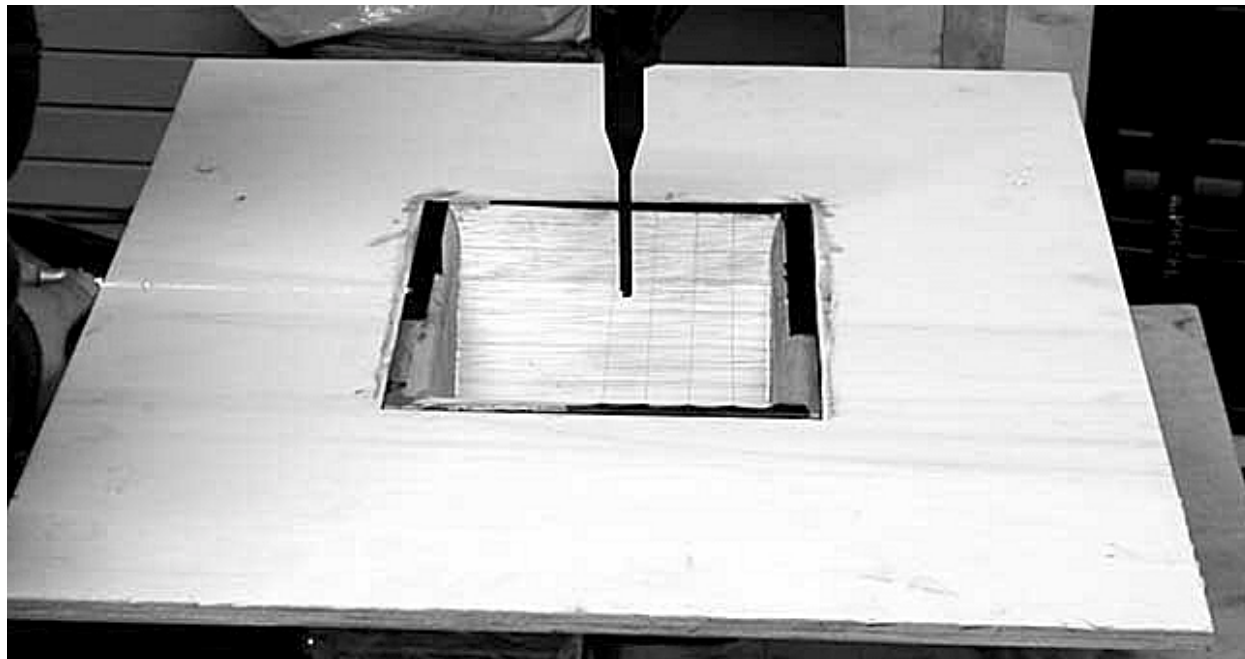


Fig. 11: How is performed the measurements throughout the mouth surface

The collection of measurement we took were elaborated by using a Matlab routine that uses measured pressure data to trace a coloured map representing the distribution of the acoustic pressure. Phase data are used to estimate time delay data in order to approximate the wavefront shape as well.

The portion of the mouth's area really measured was one quarter. The maps traced are obtained by a double mirror symmetric copy of this quarter.

An opportune window was applied at time data in order to include all the reflection that occur inside the horn, and excluding all the eventual external ones.

5. MEASURED RESULTS DISCUSSION

Midrange beaming Waist-banding and Diffraction problems

First, we wish to repropose a real world problem that we met during the optimization process of an elliptical waveguide.

We can show here improved analysis. In fact we can complete here the observation of the phenomena not only using traditional chart and pressure distribution mapping but we can even show pictures that approximate the wavefront shape measured.

As just pointed out, this reconstruction is obtained by using the phase and time information that come out of the Impulse Response measurement.

The midrange beaming problem that we first ran into, was directly correlated to the straight conical ending of this elliptical waveguide. The device was built simply using the theoretical model proposed by Geddes in Acoustic Waveguide Theory [9].

By the way, even high frequency diffraction was correlated to this. Horizontal Beamwidth characteristic is shown in figure 12.

We after showed by flaring the waveguide end that diffraction problem could be minimized, but a great advantage come with this along. The midrange beaming was also minimized, in both horizontal and vertical planes. However, some sort of high frequency directivity instability was still present and the changing is shown in figure 13.

At last we discovered that all the remaining high frequency instability was caused by the bad wavefront coherence of the driver's output. In fact, by changing the driver with a more coherent one that uses a properly designed phase plug, all the remaining instability was almost completely worked out. (Figure 14)

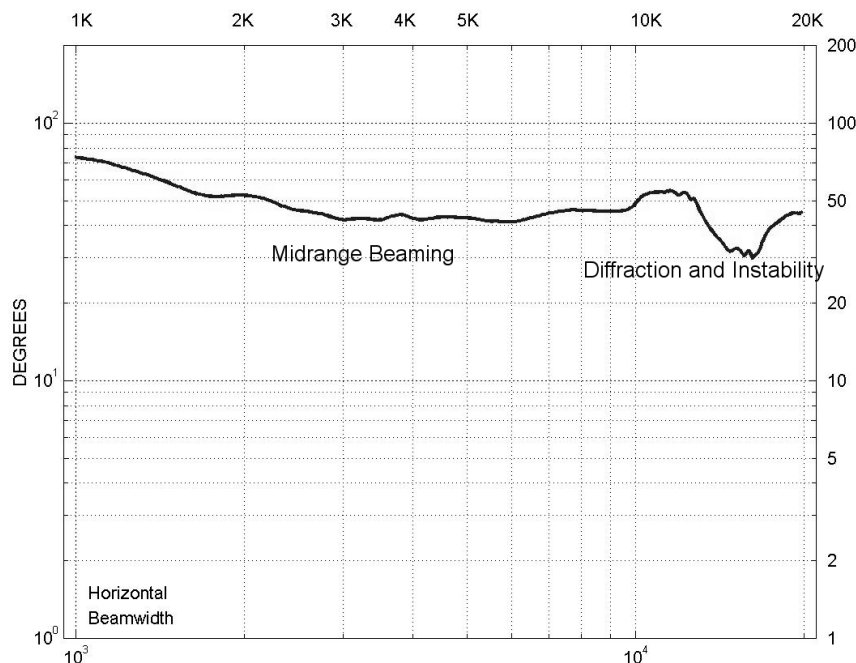


Figure 12: Horizontal Beamwidth for the conical ended waveguide

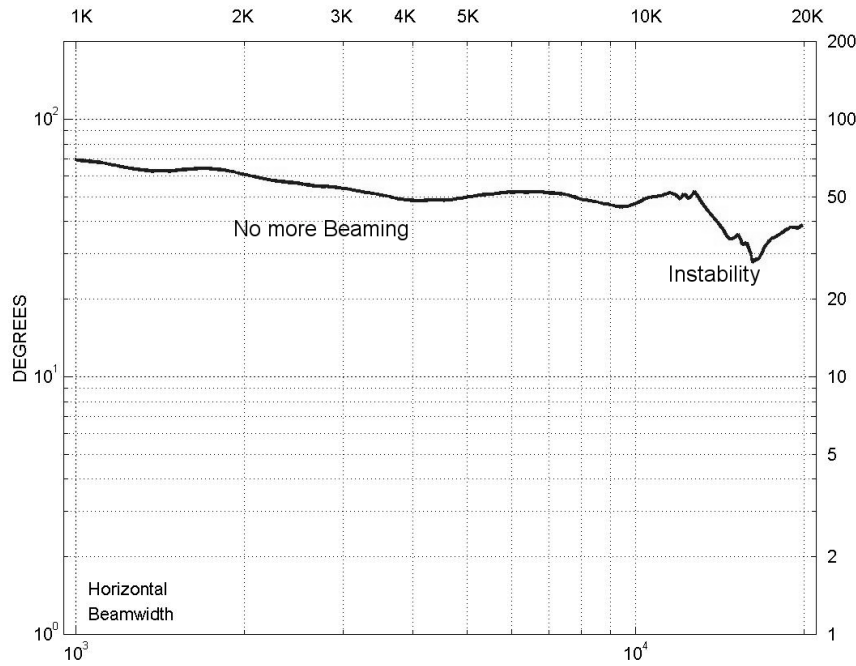


Figure 13: Horizontal Beamwidth for the flared ended waveguide

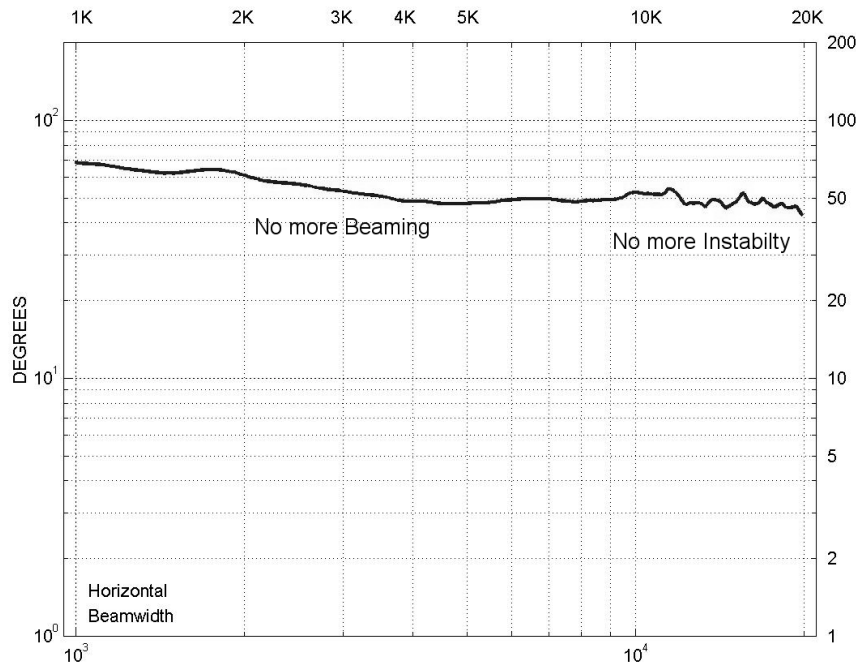


Figure 14: Horizontal Beamwidth for the same flared ended waveguide but using a better driver

The straight conical ending elliptical waveguide also shows some Waist-banding effect in the 3-5 kHz range. This showed in the polar plot in figure 15 and also resumed in a Polar Directivity Map in figure 16.

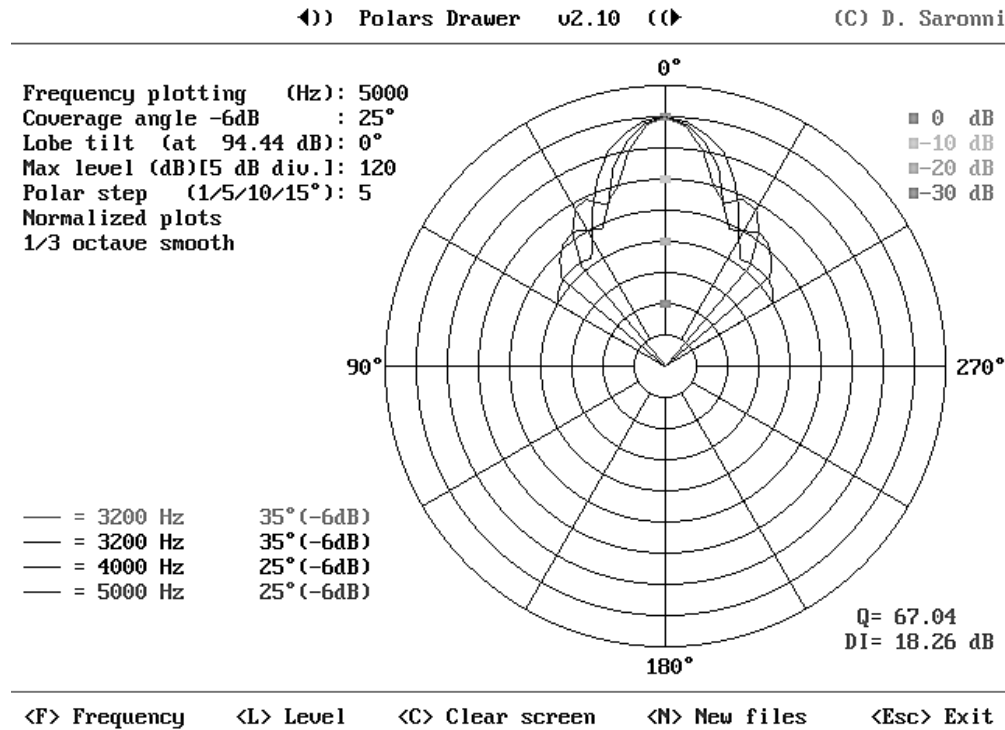


Figure 15: Waist-band energy problem in the conical ended waveguide (Vertical plane, 1/3 Oct. smoothed at 3.2kHz, 4kHz and 5kHz)

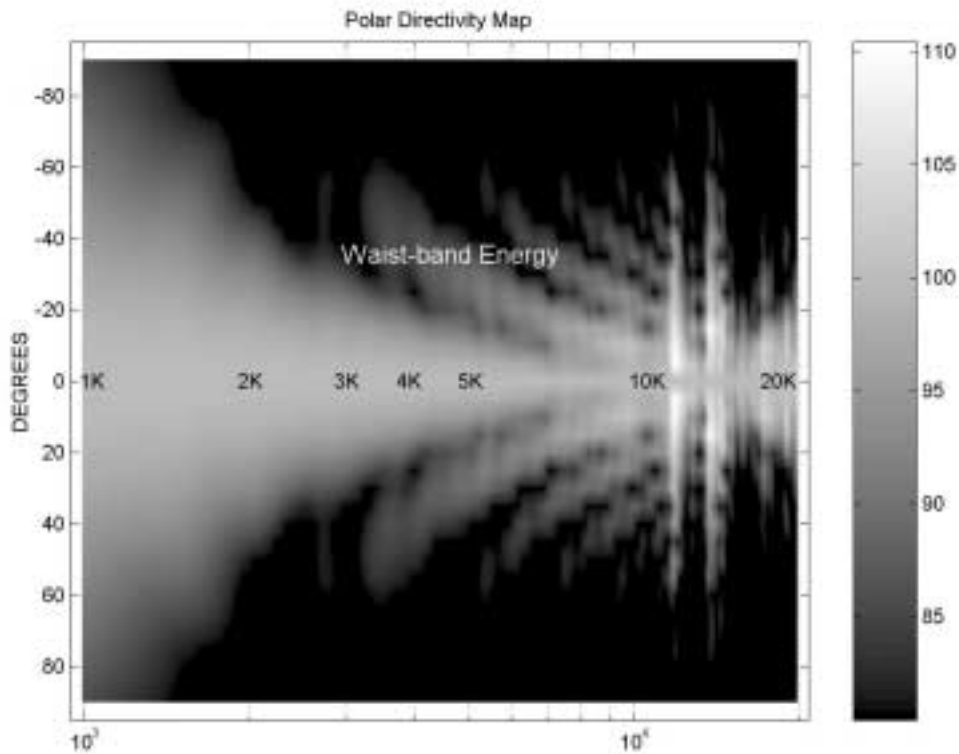


Figure 16: Waist-band energy problem in the conical ended waveguide

Now, is very interesting searching in the pressure distribution maps some evidences of all these behaviours that could help us to understand their causes.

We'd like to review the waveguides throughout the entire band mainly focusing on the conical ending waveguide.

This because it shows the most evident problems.

Here in the paper we only have black & white maps available, but could be more easy to understand what happens using the coloured ones.

Let's start with a low frequency in figure 17, where the waveguide doesn't control directivity pattern.

The pressure is well distributed and the wavefront curvature is shallow. At frequencies like this, the waveguide acts quite like a piston radiator.

As the frequency rises, we reach the horn break-up frequency where the waveguide starts to control the directivity pattern. (Figure 18)

The wavefront curvature becomes more steep and tends to take the shape of a spherical sector with the intended solid coverage angle of the waveguide.

Notice that the pressure distribution tends to dispose itself not uniformly, but assumig that of a bipole. This causes the waveguide starts to narrow its radiation.

Rising the frequency a bit more, the waveguide reaches its maximum beaming in the horizontal plane. In fact, the pressure distribution shows severe non-uniformity and the tendency to accumulate itself in some preferred positions. The wavefront shape tends to flatten back itself and to have a more complex shape, not simple as a sector of a sphere. (Figure 19).

In the 3.5-5 kHz range, some rather evident waist-banding effect is shown in figures 20, 21, 22, and 23.

Some evidences of this could be found observing how the pressure is distributed in the vertical axis of the waveguide's mouth. The pressure is accumulated in a odd number of "poles". This creates the off-axis lobes that cause the waist-banding effect just shown in figures 15 & 16 and leads the waveguide toward a very narrow beaming in the vertical axis and now the pressure distribution is accumulated in an even number of "poles". (Figure 24 and 25)

At very high frequencies the wavefront shape starts to show severe roughness.

Higher order propagation modes are probably responsible of this strange shape. (Figure 26)

At these frequencies in fact, the waveguide has internal diffraction and severe mouth diffraction as well.

It should be added to this even the fact that the driver is working in its diaphragm's break-up frequency, and at last even its poor phase plug coherency. This, as just pointed out was proven to be the main cause of the high frequency directivity instability in this design, subsequently fixed using a more properly designed driver.

Furthermore, it should be even interesting to see the behaviour presented by the flared waveguide, using a better designed driver as well, at some of the same frequencies analyzed before.

This could be found in further figures, from 27 to 33.

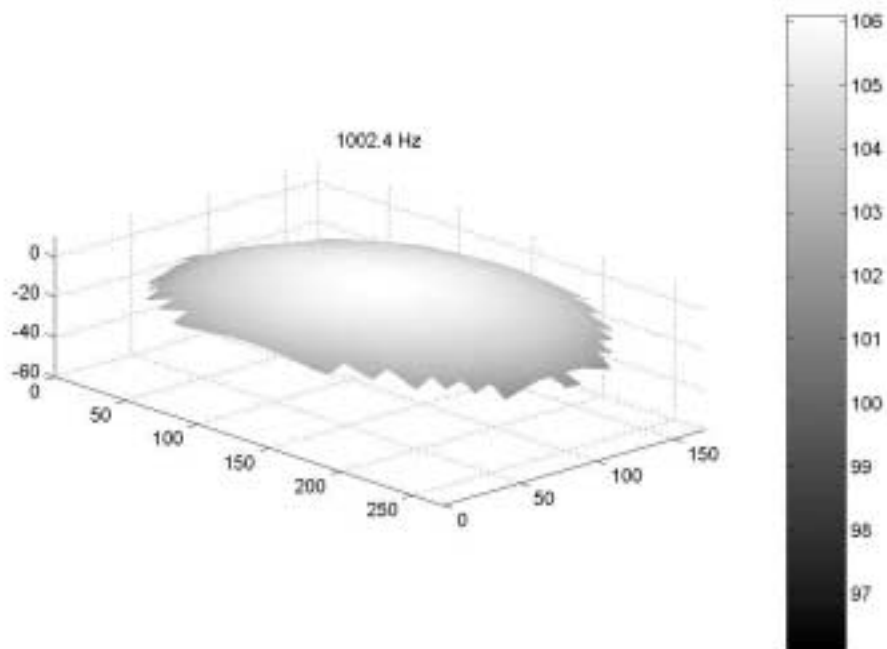


Figure 17: Pressure distribution and wavefront shape at 1 kHz (Conical ended waveguide)

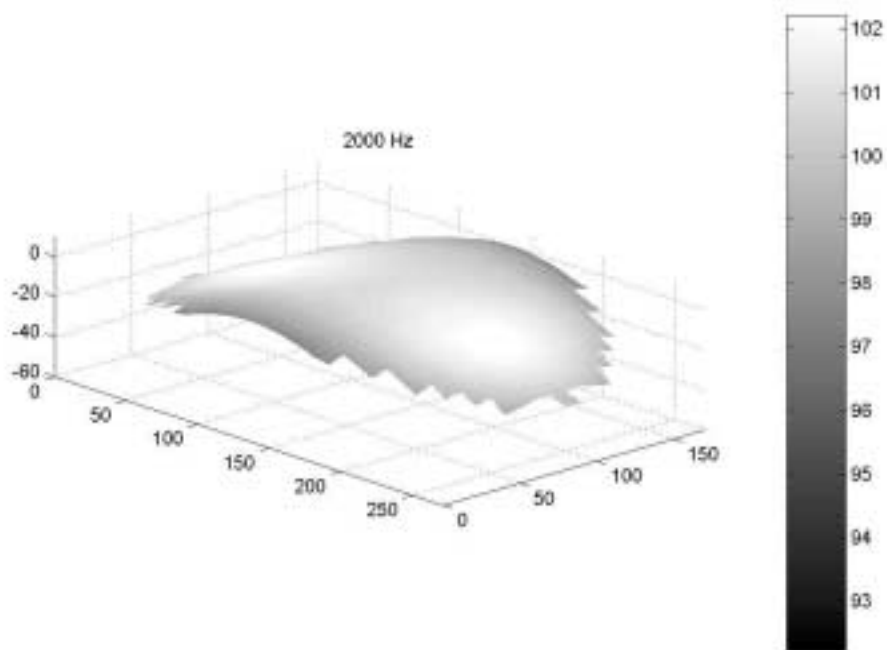


Figure 18: Pressure distribution and wavefront shape at 2 kHz (Conical ended waveguide)

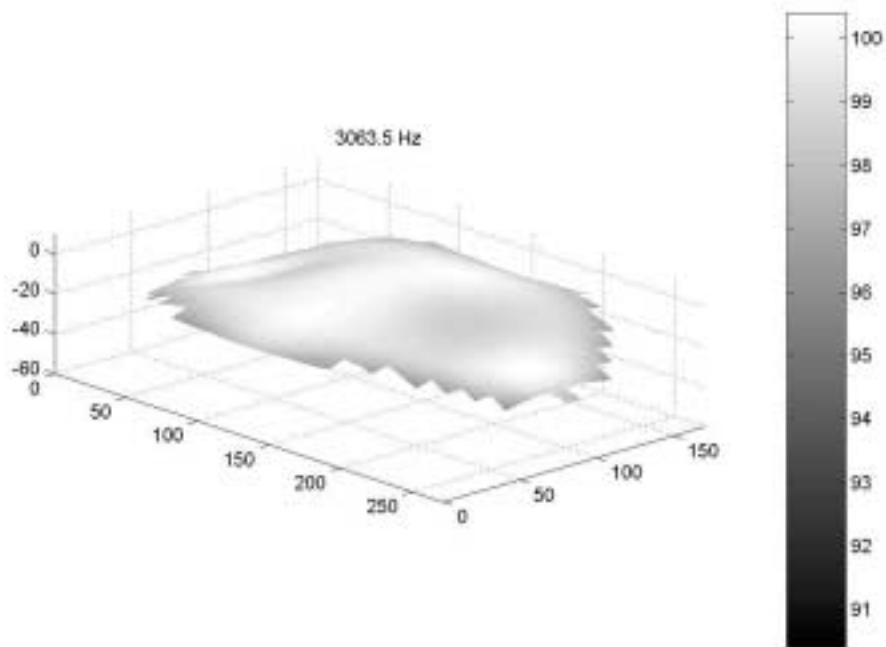


Figure 19: Pressure distribution and wavefront shape at about 3 kHz (Conical ended waveguide)

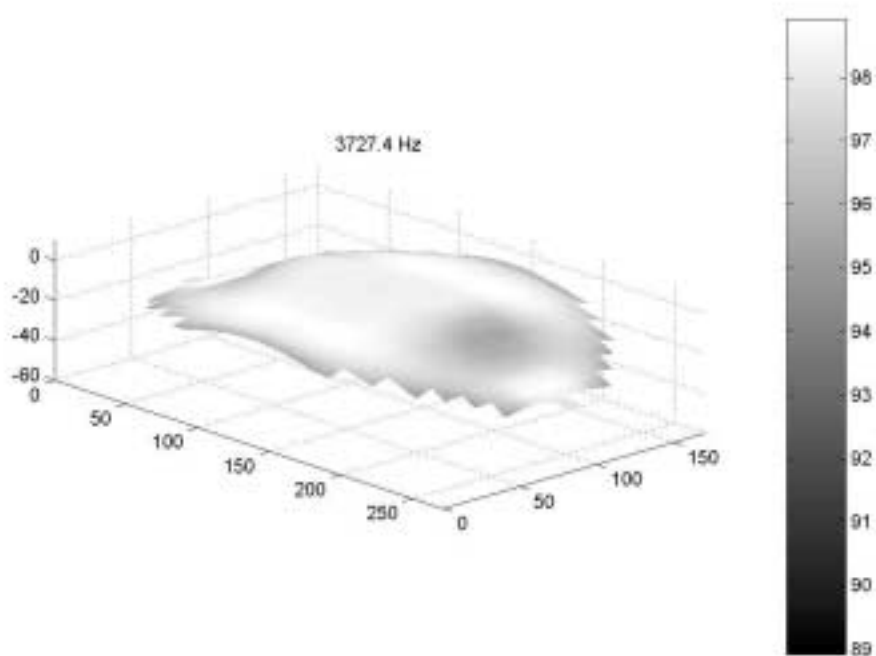


Figure 20: Pressure distribution and wavefront shape at about 3.7 kHz (Conical ended waveguide)

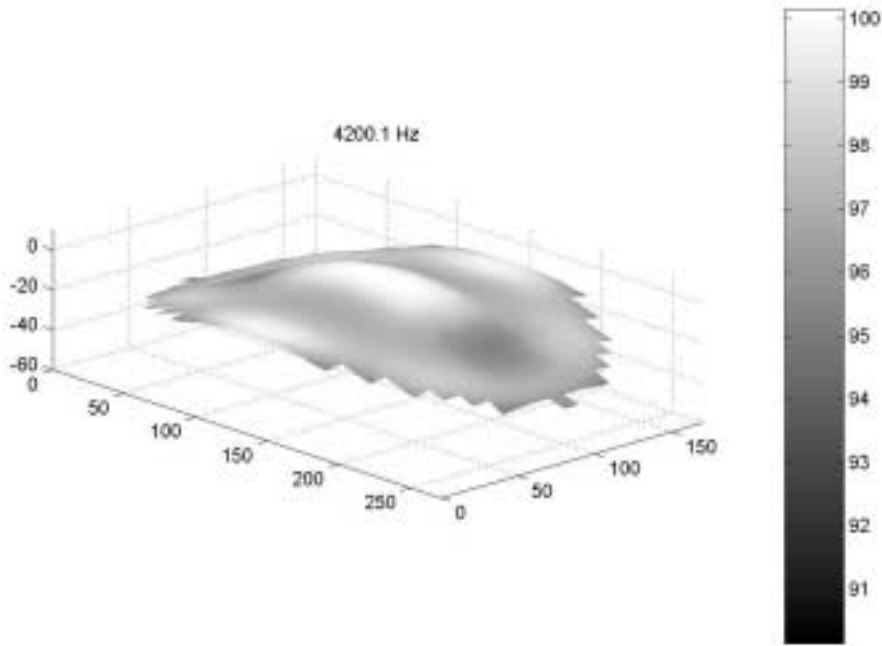


Figure 21: Pressure distribution and wavefront shape at about 4.2 kHz (Conical ended waveguide)

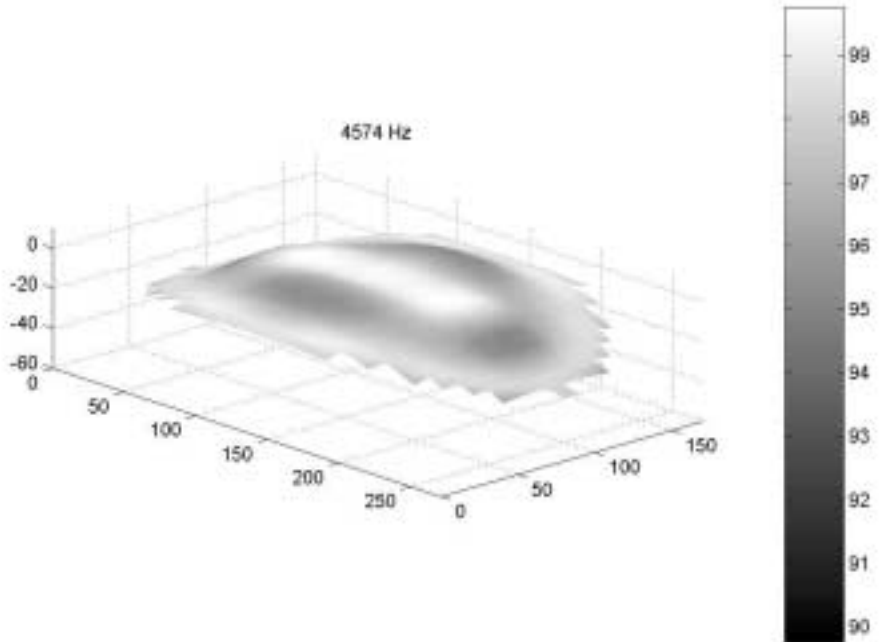


Figure 22: Pressure distribution and wavefront shape at about 4.5 kHz (Conical ended waveguide)

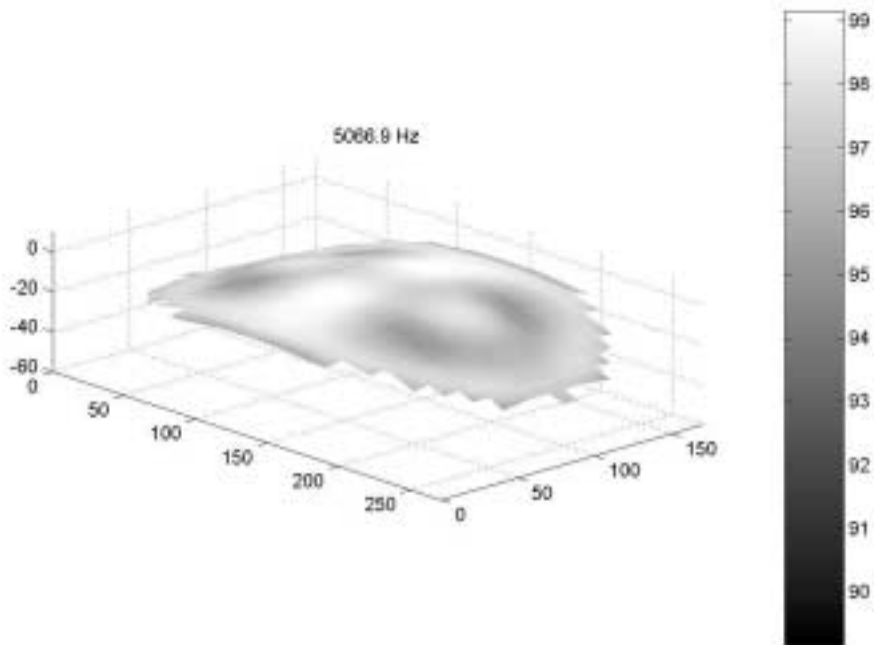


Figure 23: Pressure distribution and wavefront shape at about 5.0 kHz (Conical ended waveguide)

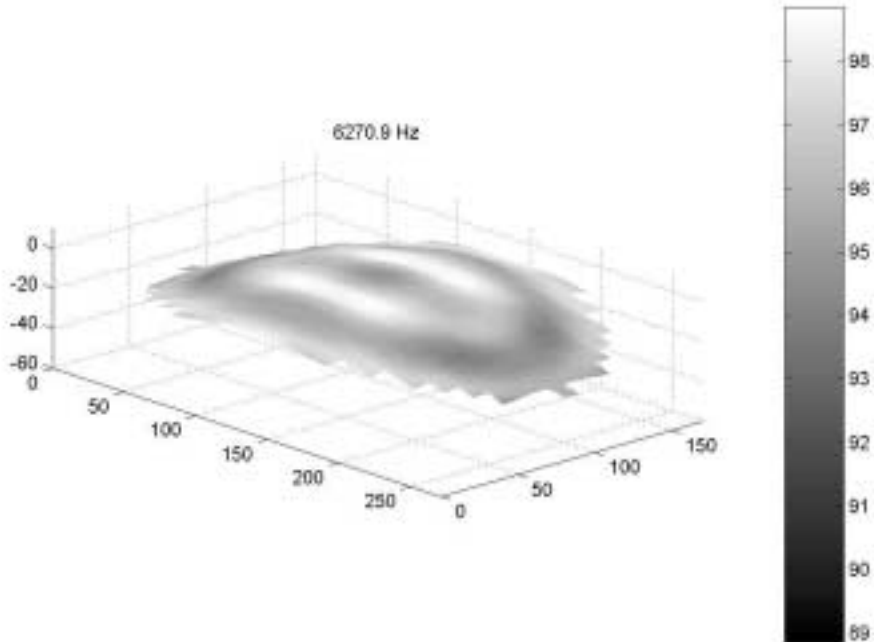


Figure 24: Pressure distribution and wavefront shape at about 6.3 kHz (Conical ended waveguide)

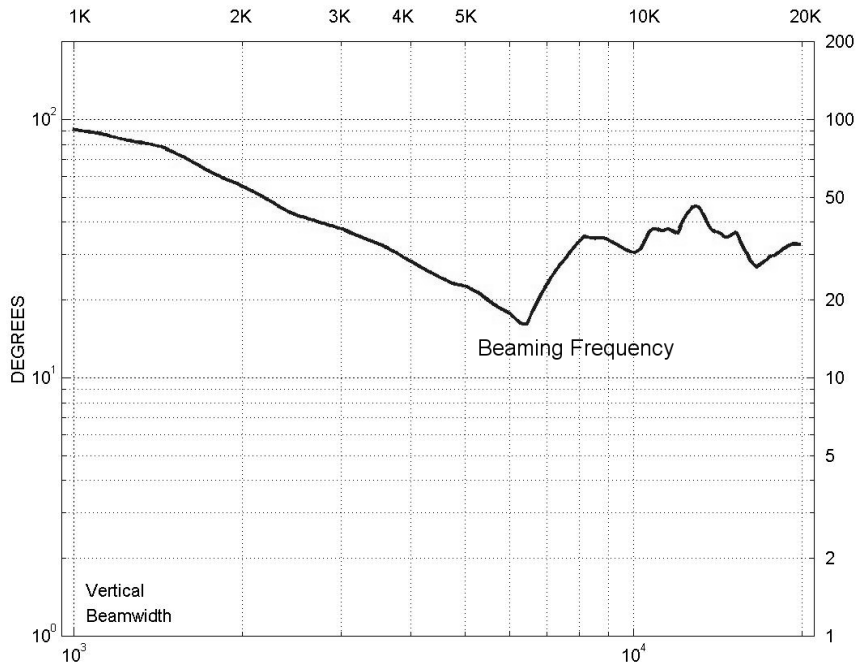


Figure 25: Vertical Beamwidth showing severe beaming around 6.3 kHz (Conical ended waveguide)

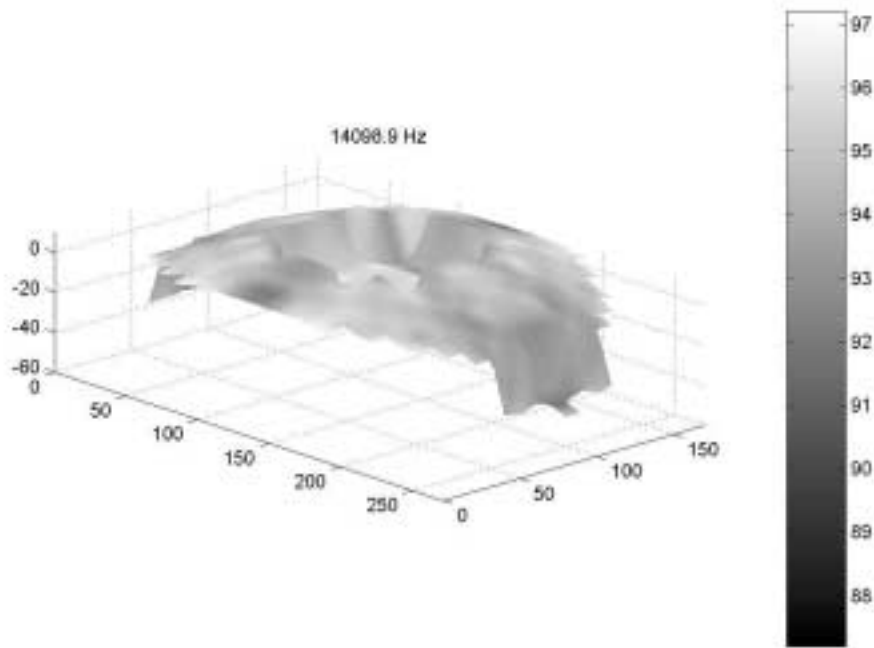


Figure 26: Pressure distribution and wavefront shape at about 14 kHz (Conical ended waveguide)

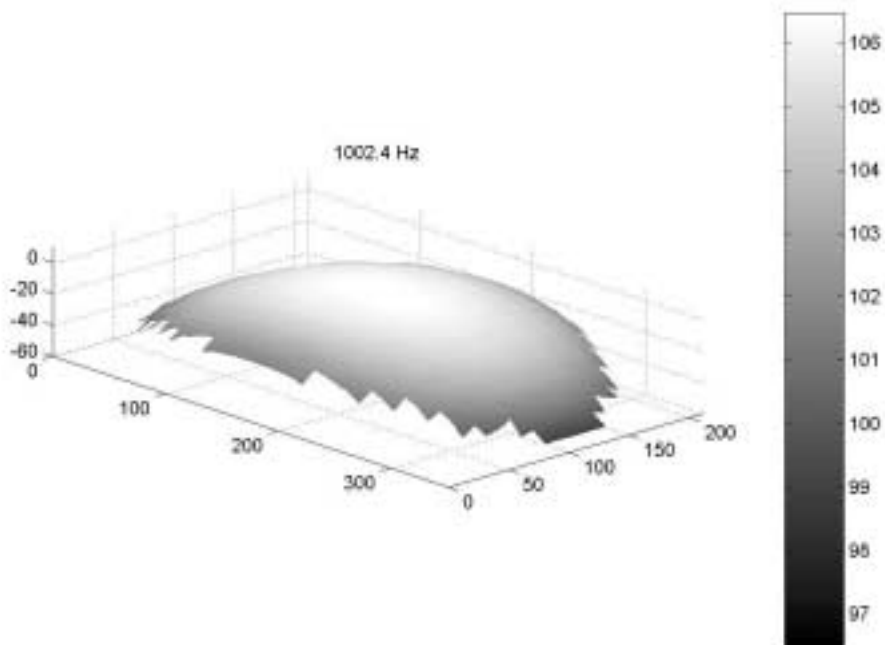


Figure 27: Pressure distribution and wavefront shape at about 1kHz (Flared ended waveguide)

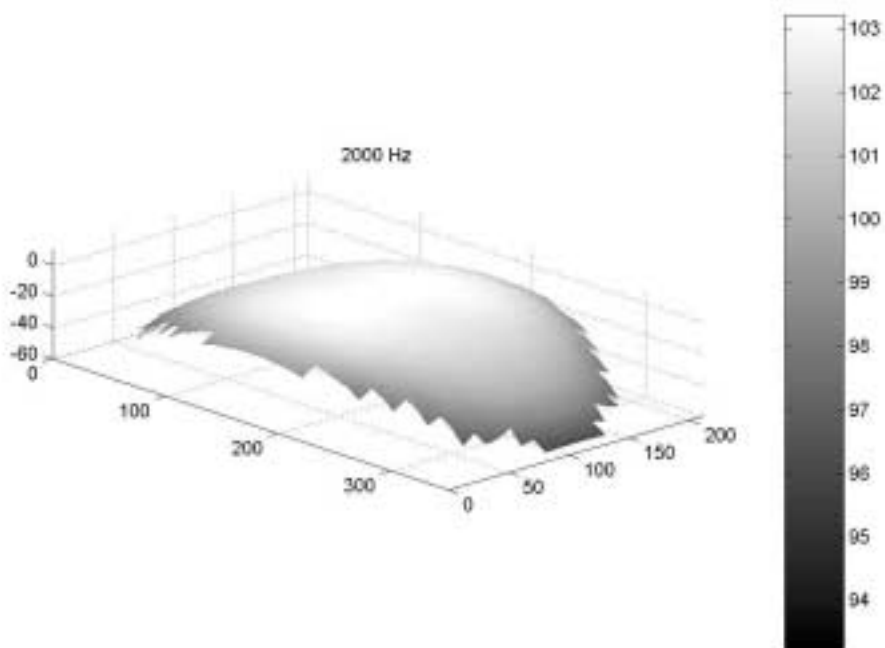


Figure 28: Pressure distribution and wavefront shape at 2 kHz (Flared ended waveguide)

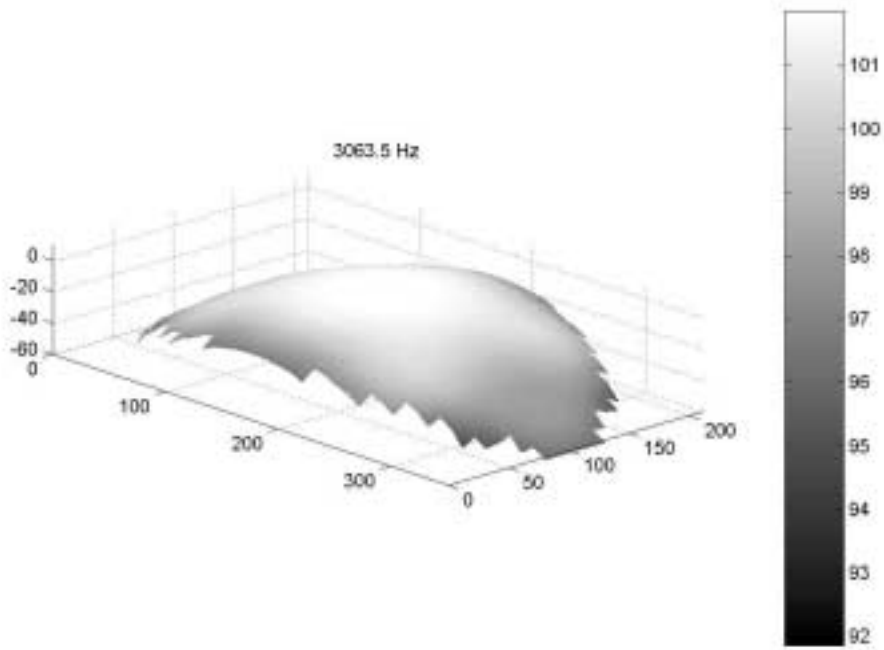


Figure 29: Pressure distribution and wavefront shape at about 3 kHz (Flared ended waveguide)

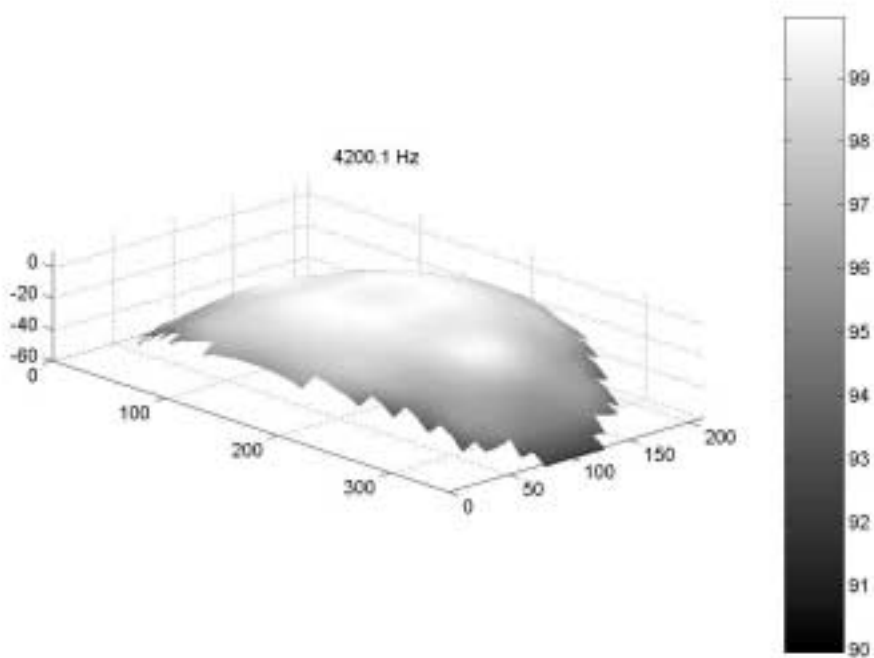


Figure 30: Pressure distribution and wavefront shape at about 4.2 kHz (Flared ended waveguide)

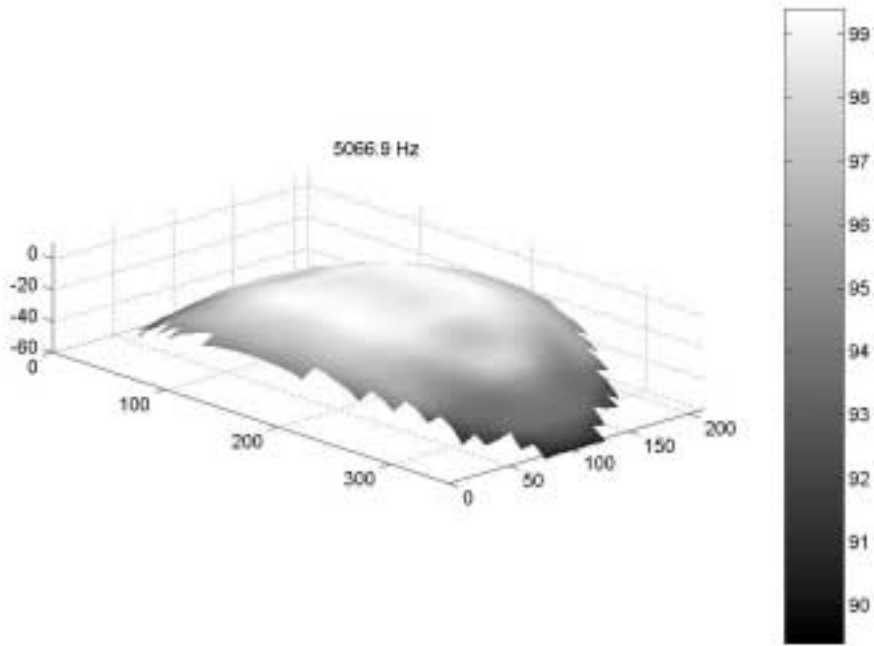


Figure 31: Pressure distribution and wavefront shape at about 5 kHz (Flared ended waveguide)

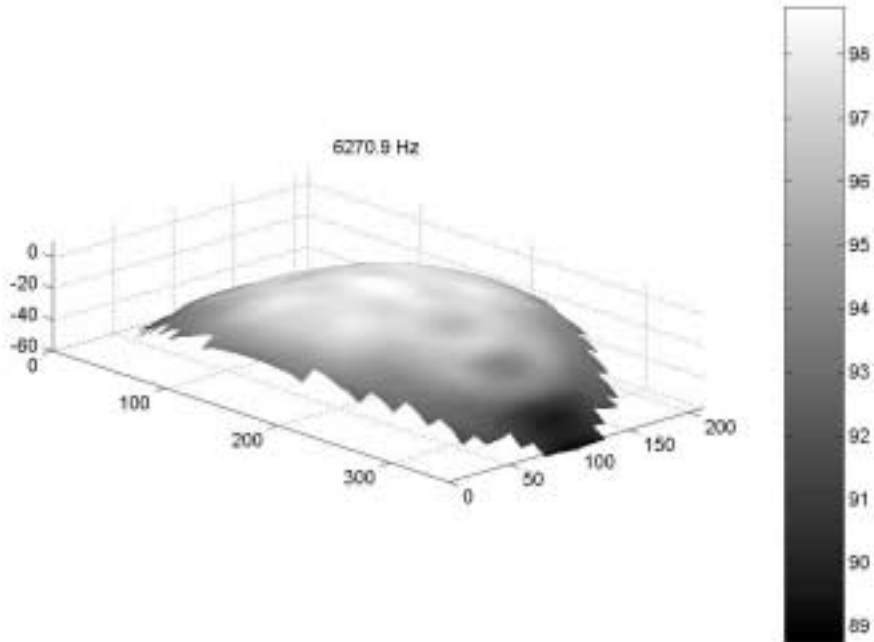


Figure 32: Pressure distribution and wavefront shape at about 6.3 kHz (Flared ended waveguide)

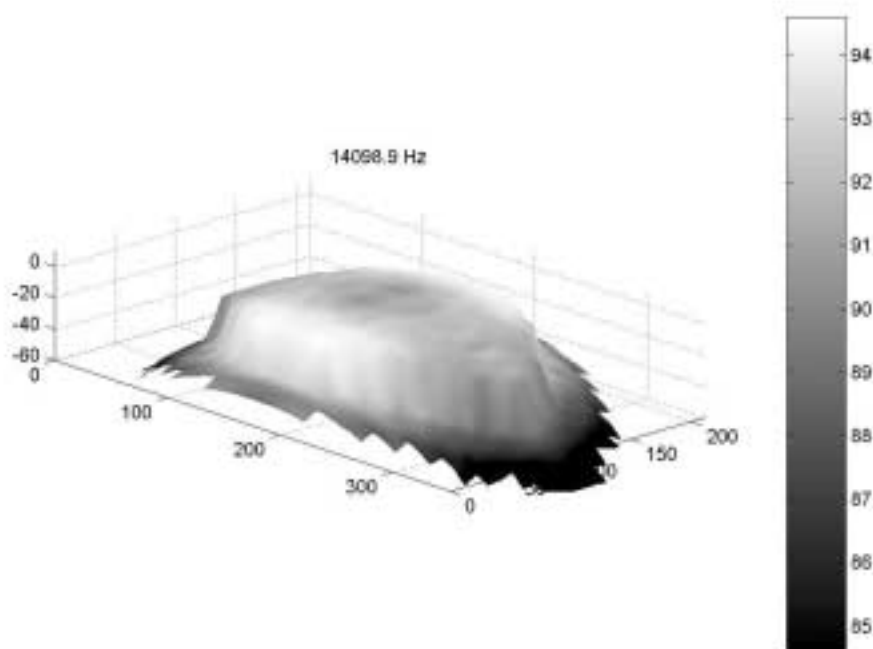


Figure 33: Pressure distribution and wavefront shape at about 14 kHz (Flared ended waveguide)

6. A SPECIFIC APPLICATION OF THIS METHOD

There is a specific field in the source's directivity and radiation characterization, as far as we are concerned, where this analysis tool could find an extremely useful application.

In fact, working with cylindrical radiation sources, it seems widely recognized that the use of traditional polar plot to characterize the radiation in the vertical plane tends to lose significance. The problem is widely regarded as one of the fundamental issues in Line Array loudspeaker systems designing and performances testing.

In fact, in order to reduce the destructive interference effects that occur when the high frequency sources' centers are not so closely spaced each other, some of the existing systems use some sort of wave former. These devices are chambers or cavities or waveguides of some sort that are claimed to shape the wavefront in some way to act as it was generated from a cylindrical source, or at least from a spherical one but with a very little vertical curvature.

So, since some of these waveformers are intended to make the wavefront to have no vertical divergence at all, it is clear that a wavefront shape "holographic" mapping method could certainly give an idea about the ability of each system in wave-shaping. With a source that is intended to have no vertical divergence, polar plots will clearly lose significance.

Moreover, the wavefront shape mapping could be useful to predict the directivity properties as well. It's shown in the following figures the behaviour of a cylindrical source that we designed lately, and that this method helped us to optimize.

We can claim this source truly cylindrical, since a constant cylindrical shape wavefront was found to be radiated along a wide band of frequencies. Here are shown, wavefront shape mapping at some different frequencies: 5, 10, 12 and 18 kHz.

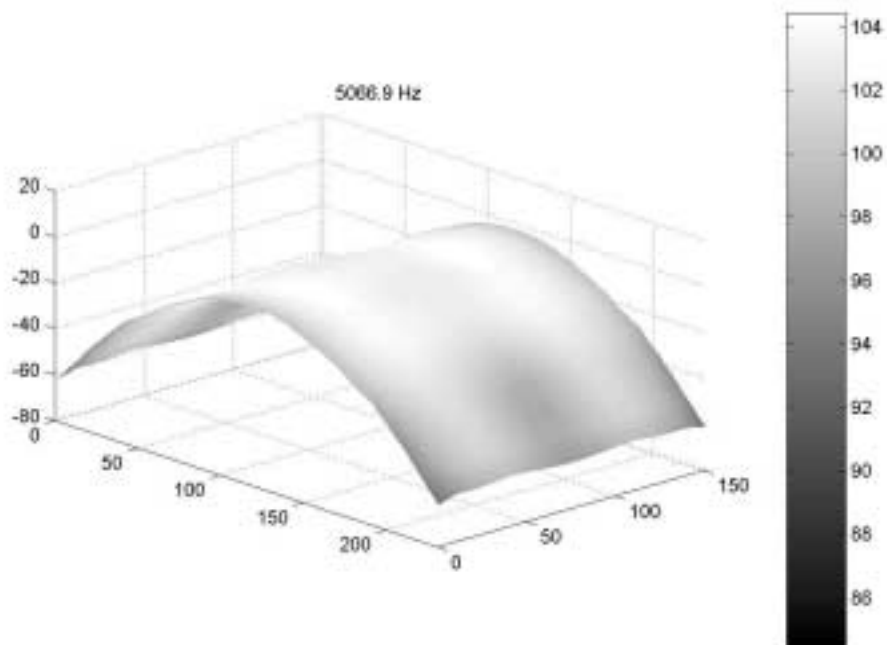


Figure 34: Pressure distribution and wavefront shape at about 5 kHz (Cylindrical Source Waveguide)

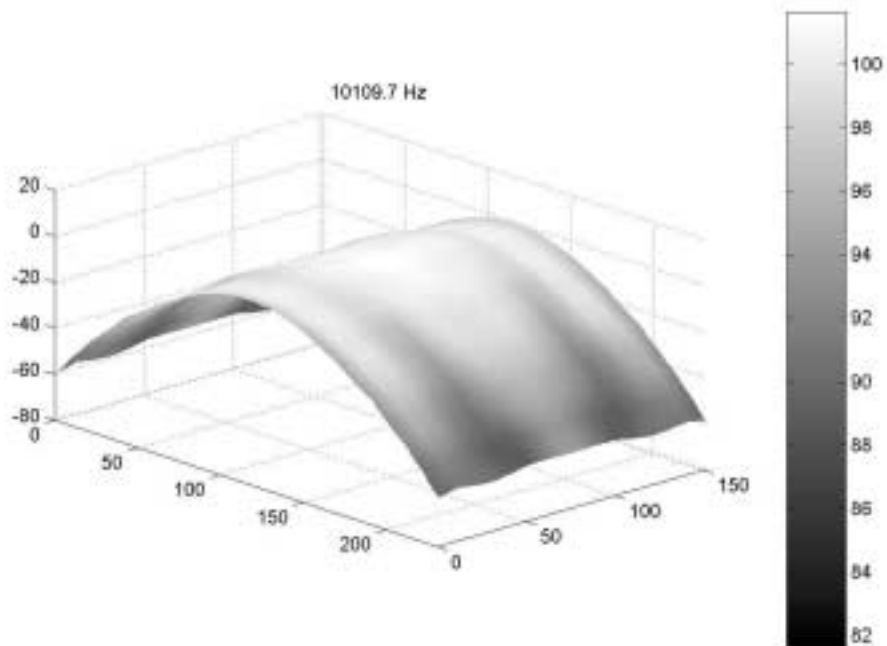


Figure 35: Pressure distribution and wavefront shape at about 10 kHz (Cylindrical Source Waveguide)

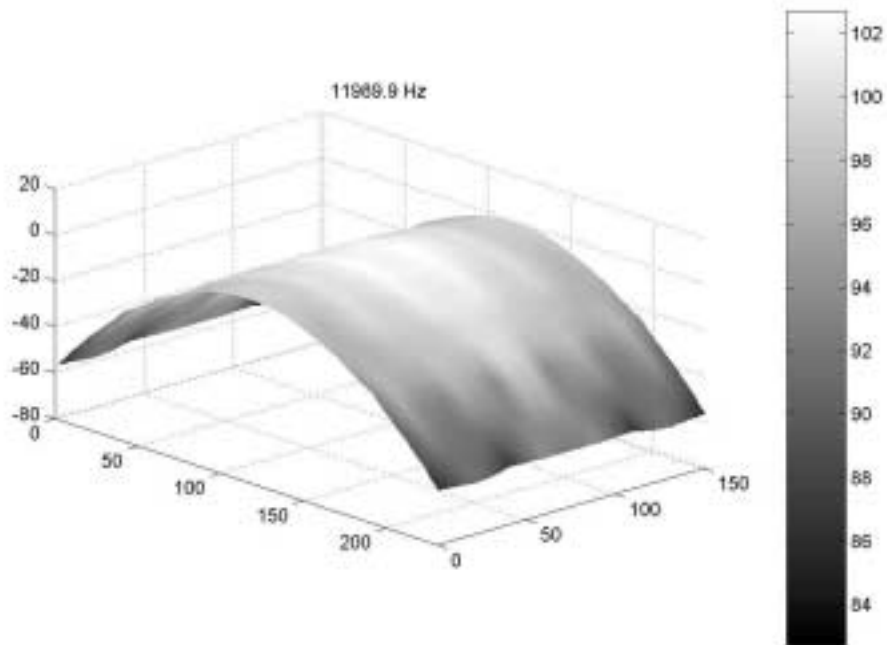


Figure 36: Pressure distribution and wavefront shape at about 12 kHz (Cilindrical Source Waveguide)

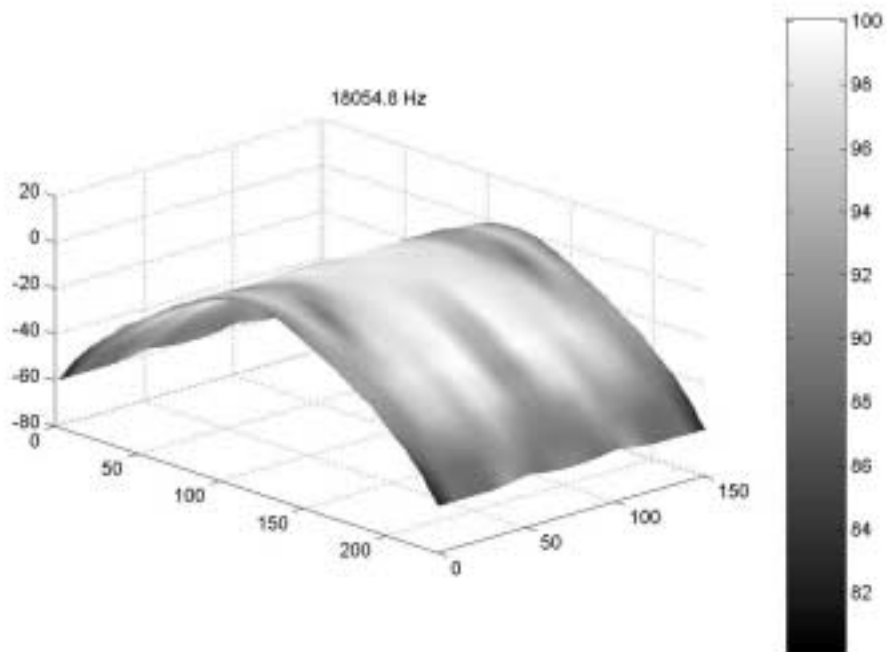


Figure 37: Pressure distribution and wavefront shape at about 18 kHz (Cilindrical Source Waveguide)

7. APPROXIMATIONS INTRODUCED

The technique we used here to show these results represents a very simple experimental method of investigation for these directivity phenomena. Could be useful to do some considerations here about the approximations introduced. These considerations were just expressed in the previous “part 1” of this work [10]

As well known, the directional properties of a radiating objects like horns could be calculated when the velocity distribution of the air's sparticles at its mouth is known.

But considering the fact that we can more easier measure the pressure: the complex sound pressure distribution across the surface of the mouth.

We must be concerned at this point to understand if the measurement of the complex sound pressure distribution could represent some sort of indirect measurement of the particle's velocity. The wave theory shows us that this quite true under some restrictions, and what is really measured is the component of the velocity in the direction of the source's axis.

Strictly speaking the propagation of sound in air is a non-linear phenomenon. But we do not usually make use of the non-linear wave equation to study sound propagation.

In fact we combine together the state equation for fluids, the equation of continuity and the linear inviscid force equation to yield a single approximated linear wave equation. In so doing, a very important fact results to be evident: the particles' velocity under some restricted condition could be considered curl-free [11].

This allow the definition of a function (ϕ) called velocity potential, making the velocity be equal to the gradient of the velocity potential. Because of this function in each point in the case of spherical waves for example is directly related to the complex value of the sound pressure, this means that the measurement of the complex pressure distribution may even indicate how the particle's velocity is distributed. The restrictions to the validity of this are the following:

- the air must be considered at the thermodynamic equilibrium
- the condensation 's' must be very very small, $s \ll 1$, that means that the sound pressure must be very small.
- this approximations are invalid in the points very close the the object's boundary

8. CONCLUSIONS AND FURTHER DEVELOPMENTS

The work showed here will clearly appear incomplete and the measurements made contains some approximation due to our rudimentary measurement setup.

This work will be certainly carried forward by us, and we are intentioned to develop the wavefront shape mapping further, in order to use these results to make calculations and prediction about the radiation of these type of sources in the far field.

This technique, has just helped us in the last times design horns and this is the reason why we would present it in this paper and share our experiences with others. We hope to be able as soon as possible to improve every procedure used here in order to yield more precision.

Moreover any improvement of the precision of such method will be useful for us to apply a similar technique to study directly driver's behaviour.

REFERENCES

- [1] D. B. Keele, Jr., "What So Sacred about Exponential Horns", presented at the 51st Convention of the Audio Engineering Society, May 1975; preprint 1038. Abstract: vol. 23, 1975 July/August.
- [2] E. R. Geddes, "Sound Radiation from Acoustic Aperture", J. Audio Eng. Soc., vol. 41, 1993 April.
- [3] Gavin R. Putland, "Every One-Parameter Acoustic Field Obeys Webster's Horn Equation", J. Audio Eng. Soc., Vol. 41, No. 6, 1993 June.
- [4a] C. A. Henricksen, M. Ureda, "Blasphemy - The Manta-Ray Horns!", presented at 58th Convention of the Audio Engineering Society, New York, November 1977; preprint 1288.
- [4b] C. A. Henricksen, M. Ureda, "The Manta-Ray Horns", J. Audio Eng. Soc., vol. 26 (1978 September)
- [5] M. Di Cola, D. Doldi, M. Furlan, "A New Approach to Waveguides", presented at 107th Convention of the Audio Engineering Society, New York, September 1999; preprint 5007.
- [6] T. F. Johansen, "On the Directivity of Horn Loudspeaker", J. Audio Eng. Soc., vol. 42 (1994 December).
- [7] J. Eargle, W. Gelow, "Performance of Horn Systems: Low-Frequency Cut-off, Pattern Control, and Distorsion Trade-offs", presented at 101st Convention of the Audio Engineering Society, Los Angeles, November 1996; preprint 4330.
- [8] D. Bie, "Vibration Resonances of Titanium Loudspeaker Diaphragm", presented at 104th convention of the Audio Engineering Society, Amsterdam, May 1998; preprint 4642.
- [9] E. R. Geddes, "Acoustic Waveguide Theory", J. Audio Eng. Soc., vol. 37 (1989 July/ Aug.)
- [10] M. Di Cola, D. Doldi, "Horn's Directivity Related to the Pressure Distribution at their Mouth", presented at 109th Convention of the Audio Engineering Society, Los Angeles, September 2000, preprint 5214
- [11] L. E. Kinsler, A. R. Frey, A. B. Coppens, J. V. Sanders, *Fundamentals of Acoustic*, 3rd ed., Wiley, New York, 1982.

RELATED READINGS

- [1] Earl G. Williams, *Fourier Acoustics, Sound Radiation and Acoustical Holography*, Academic Press, Cambridge 1999
- [2] P. M. Morse and U. Ingard, *Theoretical Acoustics*, McGraw-Hill, New York, 1968.